Journal of Fluid Science and Technology

Vol. 2, No. 2, 2007

Reduction of Fluid Torque Acting on a Rotating Disk*

Hiroyuki HANIU**, Ping WU***, Katsumi Miyakoshi** and Yoshinori YASUI****

**Department of Mechanical Engineering Kitami Institute of Technology, 165 Koen-cho, Kitami City, Hokkaido 090-8507, Japan

***Technical Division, Fuji Electric Motor Co. Ltd., 5520 Minami Tamagaki machi, Suzuka City, Mie Prefecture 513-8633, Japan

****JEOL Co. Ltd, 3-1-2 Musashino, Akishima City, Tokyo 196-8558, Japan

Email: harry@mail.kitami-it.ac.jp; Tel & Fax: +81-157-26-9224

Abstract

The flow induced energy-loss of a rotating disk in enclosed fluids bring out significant challenges in the engineering domain of high speed grinding, turbo machinery, circular saws, hard disk, and so on. Since the fluid is supplied continuously to the neighborhood of the disk surface, much of disk's rotational energy is considered to change into kinetic energy of fluid motion. In this study, a control circular cylinder was placed near the disk with its axis of symmetry coincide with that of disk to reduce the supply of flow to the disk. As a result, the fluid torque acting on the disk was found to be reduced significantly when the distance between the disk and the cylinder was intimately small. Furthermore, to measure the fluid torque directly, a new measurement method using load cell was developed in this study.

Keywords: Flow Control, Velocity Distribution, Fluid Dynamics, Fluid Torque, Rotating Disk, Kinetic Energy Loss, Load Cell, Control Cylinder

1. Introduction

Recently, along with the improvements of function and performance of industrial products, machinability of work materials becomes increasingly harder, and hence the replacement of cutting process with grinding process is considered among factories. Previously, machining efficiency of the grinding process was considered too low compared with the cutting process. However, by increasing the rim velocity of the grinder disk, advantages such as (1) improvement of ground surface smoothness, (2) remarkable improvement of machining efficiency and (3) reduction of grinding resistance, were realized. Consequently, developments of ultrahigh speed grinders were aggressively carried out[(1)]. However, in ultrahigh speed grinding, a large amount of driving energy is lost due to the friction between the rotating disk and surrounding air. This driving loss is largely due to the transfer of rotational kinetic energy of the disk into fluid momentum in tangential component. Therefore, in the ultrahigh speed grinders, high powered motors were employed and operations were done in vacuum. If the driving loss due to the fluid motion can be reduced, motor with less power can be employed or the rotational speed of a grinder can be further increased with the aid of saved energy.

Up to date, from the standing point of fluid mechanics and expected application to hard disks, there are many researches on the flow induced vibration of the rotating disk[(2 to 6)]. However, researches in relation to the fluid motion around the rotating disk and fluid torque are inadequate. In this study, a controlling method to reduce the driving loss due to fluid

*Received 17 Oct., 2007 (No. T1-05-1130)
Japanese Original : Trans. Jpn. Soc. Mech. Eng., Vol.72, No.718, B (2006), pp.1522-1528 (Received 27 Oct., 2005)
[DOI: 10.1299/jfst.2.454]

motion has been developed, and also an effort has been given to reduce the fluid torque acting on a rotating disk. Actual control method was effective, when only the disk was rotating, by placing a circular cylinder near the disk providing its axis coincide with the rotational axis of the disk to regulate the fluid supply toward the disk, and consequently reduced the fluid torque acting on the disk. The whole system from driving motor to the rotating disk, was supported by sporke made of four thin aluminum plates, and fluid torque was measured directly by a load cell composed of strain gauges attached on the support plates.

2. Experimental Set-up and Method

2.1 Experimental Set-up

The schematic diagram of the whole experimental arrangement has been presented in Fig. 1. In the present experiment, a water tank of 1000mm wide, 1545mm long and 450mm deep was used. As shown in figure, for flow visualization and LDV velocity measurement, glass plates were placed at three side walls of the tank. The depth of the water in the tank was kept to 380mm, and the water temperature was maintained at 17±2℃.

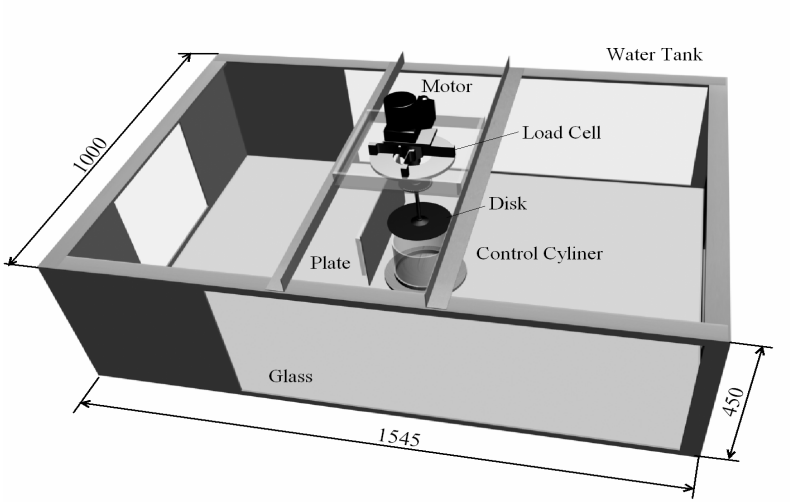

Fig. 1 Schematic diagram of the experimental arrangement

The experimental set up as shown in Fig.2 was consist of rotating disk unit, torque measuring unit, control circular cylinder unit and a flat plate likened to a work material. Further more, in order to avoid the effects of the free surface, a thin acrylic plate was placed on the water surface. The rotating disk was made of brass with diameter D=180mm and thickness t=1.5mm, and it was attached to the bottom tip of the rotational axis of 10mm diameter stainless rod by a circular brass adapter. An AC motor (Oriental motor's VW425-403T25W) with inverter rpm controller was used to drive the disk. The motor was equipped with 3:1 reduction gear head.

As shown in Fig. 3(a), the torque measuring unit was composed of aluminum bearing housing encasing ball bearing to provide disk rotation. Four load cell plates were attached to the out side of the housing. Each of the load cell plates was 1.5mm thick, 35mm wide, and 60mm long flexible aluminum plate with a strain gauge attached on it. The plates also worked as motor mount to support whole the bearing housing unit. With this configuration, torque due to mechanical friction in the bearing and gear head etc. were canceled out, and hence only the fluid torque acting on the disk could be measured.

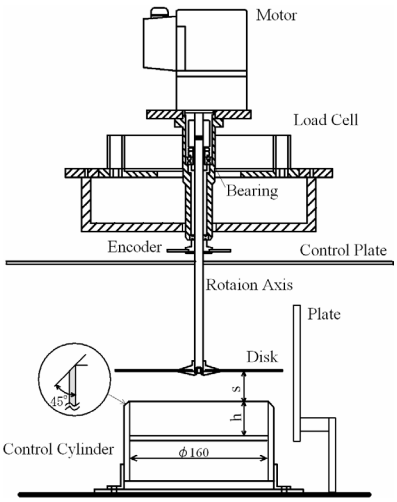

Fig. 2 Experimental set-up of rotating disk

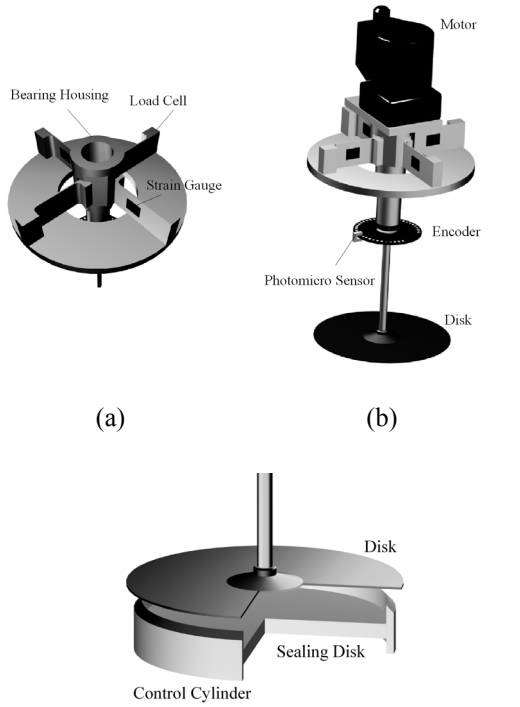

Fig. 3 Experimental arrangement of the measuring units

Torque acting on the load cell was detected by four semiconductor strain gauges and converted to voltage signal by strain meter. Prior to the torque measurement, calibration of the output voltage was done by applying known torque to the motor mount. Calibration curve for output voltage against torque is shown in Fig. 4. There is a good linearity between the torque measured by the load cell system and output voltage, and from least square analysis, the relation T=1.1E is obtained. Where, T[kgf · cm] is torque and E[V] is output voltage from the strain meter.

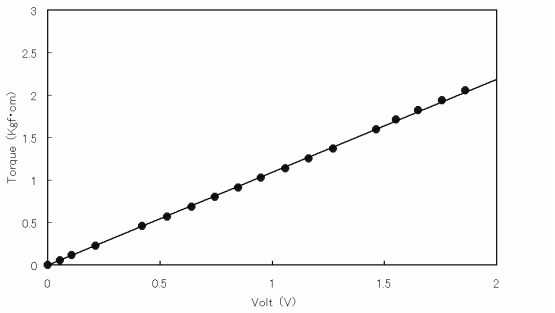

Fig. 4 Strain gauge output voltage against torque

As shown in Fig. 3(b), the rotational speed of the disk was detected by a photo micro sensor attached to slit encoder disk, and frequency of the output pulse signal was measured by a universal counter (Advantest's TR5822). By monitoring the pulse frequency, the rotational speed was manually kept constant.

The rotating disk was placed at the center of the tank and at 140mm depth. As shown in Fig. 3(c), the control cylinder was an acrylic pipe with inner diameter of d_1=160mm and outer diameter of d_2=170mm. Inner depth of the cylinder was made variable by changing the vertical position of the circular plugging disk placed inside the cylinder. Further more, in order to avoid interference between top end of the controlling cylinder and the rotating disk, outer rim of the top end of the cylinder was beveled at 45 degree. In this study, the spacing between the top end of the controlling cylinder and the bottom surface of the

rotating disk is defined as s and the depth of the controlling cylinder is defined as h, and both parameters are allowed to set at arbitrary values. These parameters were precisely set with various machine finished setting gauges. On the other hand, in the grinding operation, work material was ground on the rotating grinding stone. Therefore, in order to reproduce the state of torque measurement with presence of work material, a flat plate 400mm wide x 200mm deep with 3mm thick was also placed vertically at 1mm from the outer limb of the rotating disk.

For velocity measurements, a LDV system equipped with frequency shifters for reverse flow measurement was used.

2.2 Experimental Conditions

The torque against Reynolds number for uncontrolled flow in present study is shown in Fig. 5. Here, the Reynolds number is defined as $Re=R^2\omega/\nu$. Where R is radius of the rotating disk, ω is angular velocity, ν is kinematic viscosity of water. From the figure, increasing rate of the torque with Reynolds number is found to be enhanced when Re beyond about $3.2\text{x}10^5$. Since this value of Reynolds number is well agree with that of Kohama et al.[7], flow around the disk is considered to be in the turbulence regime for $Re>3.2\text{x}10^5$. In this study, in order to conduct torque control in fully developed turbulent flow, the Reynolds number of experiments was set to $4.6\text{x}10^5$ which is 1.4 times of the above mentioned transient Reynolds number. At this condition, the revolving speed N of the disk is 550 rpm.

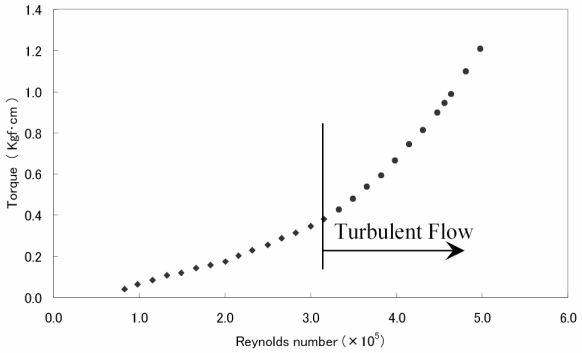

Fig. 5 Torque against Reynolds number

In the flow controlled experiment, inner diameter d_1 of the control cylinder was fixed to 160mm, outer diameter d_2 of that was fixed to 170mm, the spacing s between the bottom surface of the disk and the top end of the cylinder was varied as 0.5, 1, 2, 3, 5, 10, 15, 25, and 40mm, and the depth h of the cylinder was varied as 0, 3, 5, 7, 10, 20, 40, 60, 80, and 120mm. When the later mentioned vertical plate is placed to reproduce the presence of a work material, depth of the control cylinder was set to 7mm. The controlled torque normalized by uncontrolled torque is defined as control coefficient ε, and with this coefficient, variation of controlled torque was evaluated.

In the velocity measurement with LDV, laser beams were passed at the distance z=1.5mm bellow the bottom surface of the rotating disk. For this measurement, depth h of the control cylinder was set to 7mm, and the spacing s between the disk and the cylinder was set to 3mm. In this study, the tangential velocity component, U and radial velocity component, V were measured by aligning the optical axis of LDV with radial direction, and by orienting the optical axis perpendicular to radial direction respectively. The measuring points were varied at 5mm interval along the radial direction from the outer rim toward the center.

3. Results and Discussion

3.1 Reduction Effects of the Control Cylinder on the Disk Driving Torque

The variation of control coefficient ε against spacing s shows different trend for different depth h of the control cylinder. In order to make interpretation of the data easier, the results of torque reduction for various h were separated into four groups, such as

h=0mm, *h*=3 to 7mm, *h*=10 to 40mm and *h*=60 to 120mm, and those are shown in Figs. 6 to 9. Fig. 6 shows the torque reduction results for cylinder depth *h*=0mm. Where, control coefficient ε is taken as ordinate and spacing *s* is taken as abscissas. From the figure, no reduction of torque is made for the value of *s* larger than 10mm. However, for smaller values of *s*, the control coefficient decreases with decrease of *s*, and reaches to minimum value at *s*=2mm, then ε starts to increase as *s* further decreases. This reduction effect of the torque will be brought by the reduction of momentum transfer from the disk to fluids as the flow going to neighborhood of the rotating disk is obstructed by placing top end of the control cylinder near by the rotating disk. On the other hand, the increase of torque for the spacing *s* smaller than 2mm is considered to be originated in 0mm depth *h* of the cylinder. In this condition, bottom surface of the rotating disk and top end circular surface of the control cylinder are closing as s decreases, and Couette flow like velocity gradient will be formed in the flow between two surfaces. As a result, shear stress between the two surfaces is considered to be generated by the effect of viscosity.

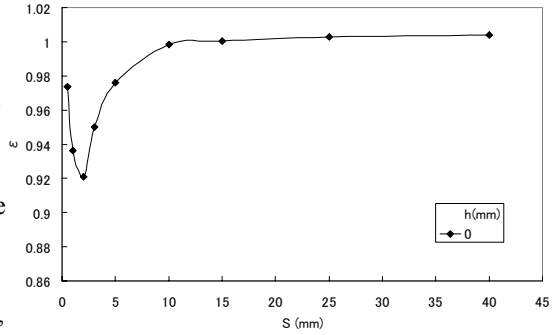

Fig. 6 Control effect for depth *h*=0mm

Fig. 7 shows control effects for cylinder depth *h*=3,5,7mm. In these conditions, maximum torque reduction by around 11% is obtained at about *s*=1mm. At this adequately small spacing of *s*=1mm, flow exchange between inside and outside of the cylinder is well reduced, and hence momentum transfer from the rotating disk to fluid was suppressed. Further more, with the increase of depth *h*, distance between the disk surface and upper surface of the plugging disk placed inside the cylinder was increased to form a basin, and hence the shear stress between two surfaces generated by the viscosity was considered to be decreased. On the other hand, torques are largely increasing in the region *s*=1 to 10mm. This is considered to be caused by increase of flow exchange between inside and outside of the cylinder. That is, part of fluids gained tangential momentum from the rotating disk, and move out from inside of the cylinder by centrifugal force, and the same volume of fluids without tangential momentum are entrained into inside of the cylinder. Due to the increase of this flow exchange between inside and outside of the cylinder, momentum transfer from the disk to fluids is increased, and hence the torque is considered to be increased. Further more, volume flux of fluid without tangential momentum taken into the inside of the cylinder is considered to be increased as the spacing *s* between bottom surface of the rotating disk and top end of the cylinder is increased. On the other hand, torques do not show increasing trend for smaller spacing such as *s*=0.5mm.

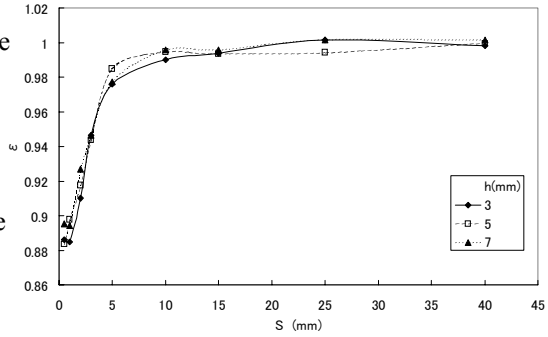

Fig. 7 Control effects for depth *h*=3,5,7mm

Fig. 8 shows control effects for cylinder depth *h*=10,20,40mm. As one can see from the figure, similar to the case of *h*=3 to 70mm, torque reduction is obtained in the region of spacing *s*<10mm, and around 8% reduction of torque is achieved at *s*=1mm. This reduction is about 2% less than the case of *h*=3 to 7mm. In-spite of reduced flow toward

the disk as the spacing between the disk and top end of the cylinder is decreased, this retreat of torque reduction effect is considered to be caused by formation of secondary flow inside the cylinder as the depth h of the control cylinder is increased. With the secondary flow, fluid motion inside the cylinder is enhanced, and inconsequently momentum transfer from the disk to the fluids inside the cylinder is increased. And the increased kinetic energy of fluids will be dissipated by viscous interaction associated with flow mixing inside the cylinder.

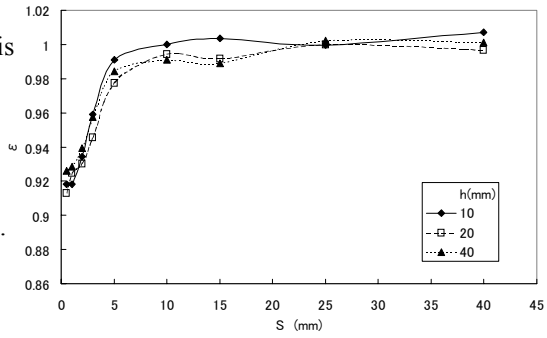

Fig. 8 Control effect for depth h=10,20,40mm

Fig. 9 shows control effect for cylinder depth h=60,80,120mm. In these conditions, the maximum torque reduction effect is obtained near s=1mm, and achieved reduction is about 4 to 6%. However, the reduction effects for s<10mm is largely subsided compared to the case of h<40mm. And for h=120mm, achieved torque reduction is merely 4% even at s<3mm. Similar to the case of h=10 to 40mm, this retreat of torque reduction effect will be caused by the increase of kinetic energy dissipation due to viscous interaction associated with the enhanced fluid motion inside the cylinder as the depth h of the cylinder is increased.

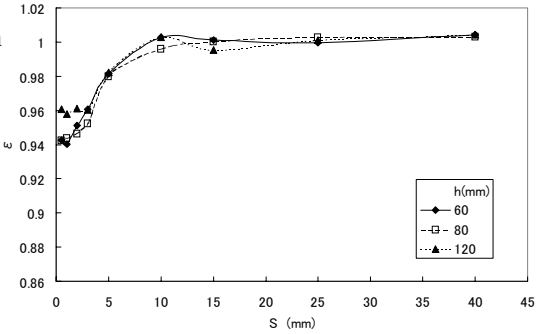

Fig. 9 Control effect for depth h=60,80,120mm

3.2 Control Effects for the Case of Placement of a Flat Plate

In the grinding process, work material is ground by a rotating grindstone. Therefore, a 3mm thick flat plate of 400mm x 200mm as work material was placed 1mm apart form the outer rim of the rotating disk, and the disk driving torque was measured. Measurements were done for the cases of with and with out control cylinder. For these measurements, depth h of the cylinder was set to 7mm where the good torque reduction effect was obtained when the plate was not placed. Fig. 10 shows variation of control coefficient ε and ε' with spacing s. Here ε' is defined as the driving torque without control cylinder divided by torque with control cylinder when the flat plate is used. As one can see from the figure, driving torque without control cylinder is increased about 4% with placement of the flat plate. This increase of torque will be caused by the increase of shear stress on the disk surface associated with the increase of velocity gradient near the disk surface as the swirling motion of the fluid near the disk is blocked by the placement of the flat plate. Therefore, for the analysis of control effect of the cylinder with placement of the flat plate, the results based on ε' have to be

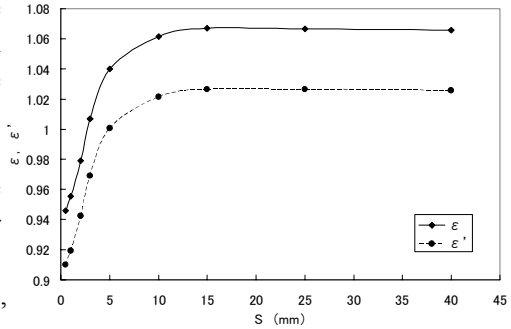

Fig. 10 Control effect with flat plate

used instead of ε. From the results of ε' in Fig. 10, torque reduction effect is obtained for the value of s smaller than 10mm even the flat plate is placed, and about 10% of torque reduction is achieved at about s=1mm. On the other hand, ε' is supposed to reach 1.0 for sufficiently large spacing. However, within the range of present experimental condition of s up to 40mm, ε' shows higher than 1.0 due to interaction between the cylinder and the flat plate.

3.3 Velocity Distributions Near the Rotating Disk Surface

Velocity components in radial and tangential direction with respect to the rotating disk were measured at 1.5mm bellow the bottom surface of the rotating disk for the values of h=7mm and s=3mm where around 11% of torque reduction was obtained. The reason to chose the value s=3mm is, for smaller spacing, placements of Laser beams become difficult and scattered light from the focus volume (LDV measuring point) does not strong enough to be detected by the receiving optics. Time mean velocity distributions for tangential component, U and radial component, V for both with and without the presence of control cylinder are shown in Fig. 11. Also, the velocity vectors for combined values of U and V of the data in Fig. 11 are shown in Fig.12 and 13. In these figures, distance from the rotating center to the measuring point is normalized by radius of the rotating disk R=90mm which is taken as abscissas. The symbols □ and ■ are showing tangential velocity component U, and the symbols ○ and ● are showing radial velocity component V. Where, open symbols stands for uncontrolled case and filled symbols stands for controlled case. In the case of uncontrolled flow, U shows a little change for r/R<0.5. For large r/R, U gradually increases and then U rapidly increases for r/R beyond 0.83. Also in the case of controlled flow, V shows similar trends to U with the increase of r/R. Estimate from the analysis of boundary layer thickness δ on disk surface[8,9] [for laminar flow: $\delta=3.22(\nu/\omega)^{1/2}$, for turbulent flow: $\delta=0.522r(\nu/\omega r^2)^{1/5}$], δ is expected to be about 0.44mm at r/R=0.45 where laminar flow is likely to be formed, and about 2.6mm at r/R=1.0 where fully turbulent flow is likely to be formed. Therefore,

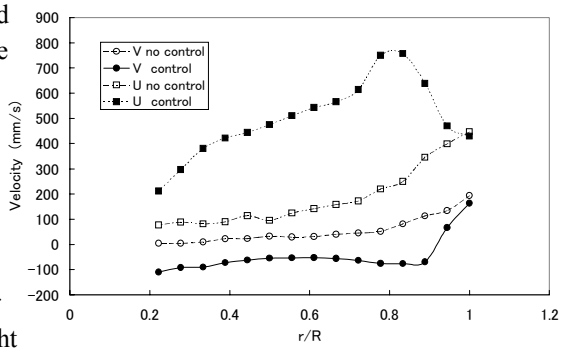

Fig. 11 Mean velocity distributions

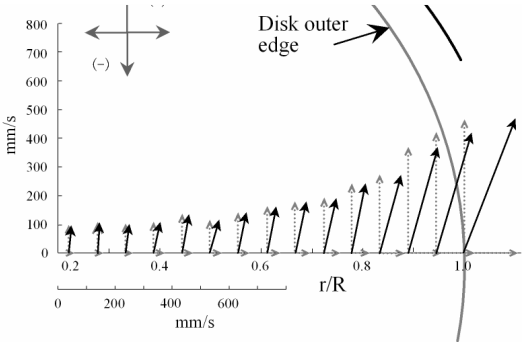

Fig. 12 Uncontrolled mean velocity vectors

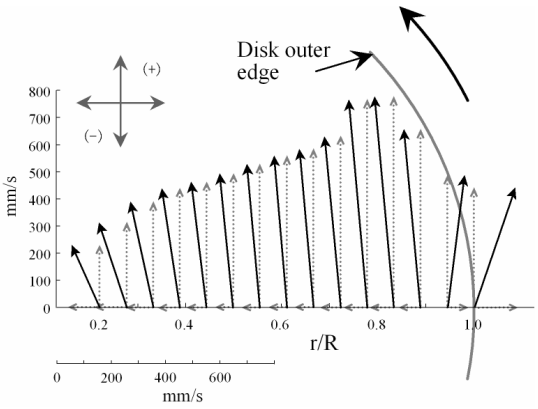

Fig. 13 Controlled mean velocity vectors

observed U and V will be showing velocity outside the boundary layer near r/R=0.5, and will be showing velocity inside the boundary layer near r/R=1.0. On the other hand, when z=1.5mm is normalized by r, z/r=0.167 at the outer rim of the rotating disk, and measured velocities are about U=450mm/s and V=200mm/s, and hence the velocity ratio V/U is 0.444. Kohama et al.[7] studied in detail a boundary layer on a disk 400mm diameter rotating in air. From their velocity distribution in fully turbulent region at Re=7.76x10^5 near outer rim of the disk, velocity ratio V/U was estimated as 0.395 at z/r=0.0167. Therefore, present result is considered to well agree with that of the previous study[7].

In the case of flow control with the cylinder, tangential velocity component U becomes 2 to 5 times larger than the case of without flow control. By placing the control cylinder sufficiently close to the disk, flow exchange between inside and outside the cylinder is obstructed, and the fluids gained tangential momentum from the rotating disk hardly flow to outside the cylinder. Therefore, the momentum will be stored inside the cylinder, and hence the velocity must be increased. Further more, the maximum velocity is located at a little inside the inner wall of the cylinder (r/R=0.89), and this will be caused by the effect of boundary layer on the inner wall of the control cylinder. Besides, at outside the cylinder near the outer rim of the rotating disk, velocity is about the same value as the case of uncontrolled flow. In contrast, radial velocity component V for the case of controlled flow shows opposite negative value to the case of uncontrolled flow, and this is indicating the presence of flow toward the center of the rotating disk. This is because a secondary flow is formed within the nearly closed chamber by the placement of the control cylinder, and the negative velocity is sensed at the measuring point 1.5mm from the rotating disk. Otherwise, the measuring point is already outside the boundary layer, and then sensing the flow coming into the inside of the cylinder. In order the fluids gained momentum from the rotating disk inside the cylinder to move out, even in very small amount, from the continuity, there must be flow coming into the inside of the cylinder. The study of Kohama et al. shows that the boundary layer on the rotating disk is fairly thin as well as would be in the present experiment. Therefore, outside the boundary layer, velocity of the outgoing fluid could not be detected but incoming flow from the outside or circulating flow inside the chamber must be detected. But, detail of flow situation was not known yet because flow visualization was unable to conduct. RMS values of velocity fluctuation for both the controlled and uncontrolled flow are shown in Fig.14. Here the RMS values are normalized by the outer rim solid velocity of the disk. RMS values are higher in the case of controlled flow than the case of uncontrolled flow for both tangential component U' and radial component V', and hence the turbulence level is enhanced when flow is controlled by the cylinder.

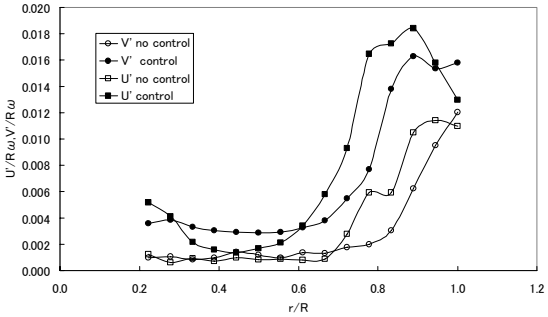

Fig. 14 RMS velocity distributions

In the case of uncontrolled flow, turbulence levels (RMS value) are higher at the outer rim portion than the center portion, namely the turbulence levels start to increase near r/R=0.7, and rapidly increase from r/R=0.8 to outer rim. Comparing to the mean velocity distributions, turbulence level was found to increase with increase of mean velocities. This rapid increase of turbulence level will be associated with the change of flow regime from transition to fully turbulent. On the other hand, for r/R less than 0.7, similar to the mean velocity, turbulence levels do not show significant change and stay calm. And in the transition regime and inner portion, turbulence level is significantly small and nearly uniform.

In the case of controlled flow, velocity fluctuation in radial component V' shows small change in turbulence level and it remains nearly uniform for r/R up to about 0.6. However, for r/R beyond 0.6, turbulence level is rapidly increasing toward the outer rim of the control cylinder. In the case of uncontrolled flow, disturbed flow is immediately taken away from the disk. However, in the case of controlled flow, turbulence level is enhanced because the disturbance inside the cylinder is stored and recirculates within the cylinder, and also the mean velocity increases inside the cylinder, and more over in coming and out going flows are interacting. On the other hand, turbulence level near the center of the disk is increasing. The fluids coming into inside the cylinder through the clearance between the disk and the cylinder will gain disturbance from interaction with the out going fluid, and then the incoming fluid is carried toward the center of the disk by the secondary flow. Inconsequently, disturbed flow will be supplied toward the disk center along the rotating axis.

4. Conclusions

Suppression of fluid torque acting on a rotating disk with a circular cylinder was attempted and the following useful results were obtained.

(1) By closely placing a circular cylinder to a rotating disk, fluid flowing toward the disk along the rotational axis was prevented, and inconsequence, fluid torque was suppressed due to reduction of momentum transfer from the disk to fluid.

(2) By placing a circular cylinder very close to the disk providing the depth of the cylinder sufficiently small, formation of secondary flow inside the circular cylinder was prevented and flow exchange between inside and outside the cylinder was reduced. As a result, momentum transfer from disk to fluid is further reduced, and fluid torque was as well further suppressed.

(3) At the condition torque is reduced, time mean velocities and turbulence levels are significantly increased, and the velocity distributions along the radial direction were also drastically changed in contrast to the uncontrolled case.

Nomenclature

D: disk diameter (180mm)
d_1: inner diameter of control cylinder (160mm)
d_2: outer diameter of control cylinder (170mm)
E: output voltage from load cell
h: depth of control cylinder
N: revolving speed of disk (rpm)
Re: Reynolds number ($R^2 \omega / \nu$)
R: radius of disk
r: radial coordinate with respect to disk
s: spacing between disk and control cylinder
T: fluid torque
t: thickness of disk
z: coordinate normal to disk surface
ε: control coefficient of torque
ε': control coefficient of torque with flat plate
ν: kinematic viscosity
ω: angular velocity of disk (radian/sec)

References

(1) Inada, Y. et al., Development of Wheel Spindle for Ultra-High Speed Grinding Machine-Studies on Ultra-High Speed Grinding (1st Report)-, Seimitsu Kogakukaishi (Journal of the Japan Society of Precision Engineering), Vol.62, No.4 (1996), pp.19-23.

(2) Humphrey, J.A.C. et al., Unobstructed and Obstructed Rotating Disk flows: A Summary Review Relevant to Information Storage Systems, *Advances in Information Storage Systems*, Vol.1 (1991), pp.79–110.

(3) Renshaw, A. A. et al., Aerodynamically excited vibration of a rotating disk, *Journal of Sound and Vibration*, Vol.177, No.5(1994), pp.577–590.

(4) Huang, F. Y., and Mote, C. D., Jr., Mathematical Analysis of Stability of a Spinning Disk Under Rotating, Arbitrarily Large Damping Forces, *Transaction of ASME, Journal of Vibration and Acoustics*, Vol.118 (1996), pp.657-662.

(5) Moroi, T. et al., Viscoelastic Flow due to a Rotating Disk Enclosed in a Cylinder Casing (High Viscous Silicone Oil), *Nihon Kikai Gakkai Ronbunshu, B(Transaction of the Japan Society of Mechanical Engineering, Series B)*, Vol.66, No.647(2000), pp.1691-1697.

(6) Kang, N. and Raman, A., Aeroelastic Flutter Mechanisms of a Flexible Disk Rotating in an Enclosed Compressible Fluid, Transactions of the ASME, Journal of Applied Mechanics, Vol.71 (2004), pp.120-130.

(7) Kohama, A. et al., Traveling Disturbance on a Spinning Disk Boundary Layer., *Nihon Kikai Gakkai Ronbunshu, B(Transaction of the Japan Society of Mechanical Engineering, Series B),* Vlo.60, No.574 (1994), pp.1978-1984.

(8)Schlichting, H., Boundary-Layer Theory(1968), pp.606-607, McGraw-Hill.

(9) Ikui, T. and Inoue, M., Viscous fluid Dynamics(in Japanese)(1985), pp.164-167, Rikogakusha Publishing Co..